Corrosion Science 99 (2015) 205–218

Contents lists available at ScienceDirect

Corrosion Science

journal homepage: www.elsevier.com/locate/corsci

A double-cylinder model incorporating confinement effects for the analysis of corrosion-caused cover cracking in reinforced concrete structures

Ray Kai Leung Su, Yanlong Zhang*

Department of Civil Engineering, The University of Hong Kong, Pokfulam Road, Hong Kong

ARTICLE INFO

Article history:
Received 17 April 2015
Received in revised form 17 July 2015
Accepted 24 July 2015
Available online 27 July 2015

Keywords:
A. Steel reinforced concrete
B. Modelling studies
C. Rust

In this paper, a double-cylinder model with a consideration of concrete confinement effects is proposed to simulate reinforcement corrosion-caused cover cracking. The analytical model incorporates force equilibrium in both tangential and radial directions as well as volume expansion and deformation compatibility in the steel-rust-concrete interface. Confinement effects outside the cylinders are taken into account by comparing the numerical and available experimental results. Parametric studies are conducted to investigate the variations of the critical volume of consumed steel, critical expansive pressure and time to cover cracking.

1. Introduction

The corrosion of reinforcing bars in concrete has been identified as one of the major worldwide deterioration mechanisms for reinforced concrete (RC) structures [1,2], which can significantly affect the serviceability, durability and strength of such RC structures [2]. Damage to concrete due to corrosion-caused expansive pressure can lead to cracking and even spalling of the surrounding concrete. It is imperative, therefore, to understand the mechanism of corrosion-induced cover cracking and to provide a theoretical model for the structural integrity and lifetime analysis of RC structures. Moreover, in order to make appropriate decisions regarding the structural inspection, strengthening, repair, replacement and demolition of old RC structures, knowledge of the amount of reinforcing steel lost, the corrosion-caused expansive pressure and the remaining lifetime of such RC structures is essential.

In recent decades, various analytical models [1–24] have been developed to simulate the corrosion of RC structures. Bažant [5] proposed a uniform-cylinder analytical model with a homogeneous linear elastic material to simulate reinforcement corrosion-induced cover cracking. The model was modified by Liu and Weyers [1] to account for a porous zone around the steel-concrete interface in which the corrosion products needed to be filled prior to the development of expansive pressure to the concrete cover. Based on this model, EI Maaddawy and Soudki [6] predicted the time from corrosion initiation to concrete cracking. Papakonstantinou and Shinozuka [3] further extended EI Maaddawy and Soudki's model [6] to simulate all stages of RC corrosion, including corrosion initiation, crack initiation and propagation.

Tepfers [7] proposed a double-cylinder model in which the cylinder was divided into uncracked and cracked parts. Many researchers attempted to improve this model by taking into account the residual tensile strength in the cracked concrete. Wang and Liu [8–9] assumed that the concrete in the cracked cylinder was an isotropic linear elastic material with an elastic modulus equal to that of the outer cylinder. Based on this model, Han et al. [4] examined the process of the degradation of flexural strength in RC concrete members caused by steel corrosion. Bhargava et al. [2,10–12] postulated that the concrete in the cracked cylinder was an isotropic linear elastic material with a reduced elastic modulus compared to that of the outer uncracked concrete cylinder. Balafas and Burgoyne [13] proposed a double-cylinder model based on the fracture mechanics theory to determine structural lifetime from corrosion initiation to cover spalling. Li et al. [14–15] assumed that the cracked concrete cylinder was an isotropic material with a reduced elastic modulus in the tangential direction. However, the stress continuity and strain compatibility conditions on the common boundary between the uncracked and cracked concrete cylinders were not satisfied in their model. Chernin et al. [16] extended the double-cylinder model by adopting a consistent stress-strain relationship for both uncracked and cracked concrete cylinders and ensured the continuity of stress and strain on the

* Corresponding author.
E-mail address: ylzhang200@gmail.com (Y. Zhang).

http://dx.doi.org/10.1016/j.corsci.2015.07.009
0010-938X/

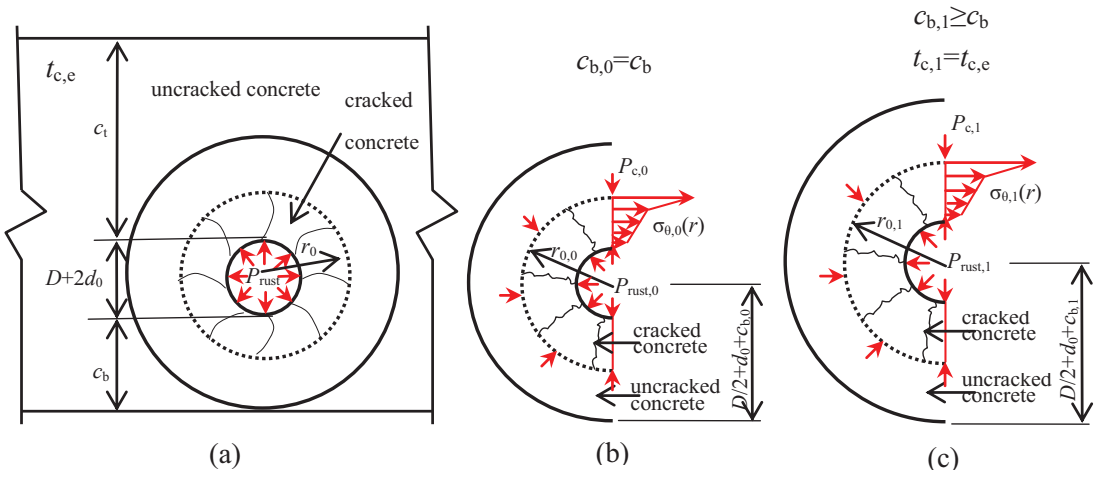

Fig. 1. The corrosion problem: (a) the actual case, (b) the traditional analytical model, and (c) the proposed analytical model.

common boundary between the two cylinders. Kim et al. [17] developed a model to explore realistic mechanical properties of the corrosion layer, including the pressure-free corrosion strain and the stiffness of the corrosion layer, with the consideration of corrosion products penetrating into the concrete pores and cracks around a steel bar. Zhao et al. [18] derived a model using elastic mechanics to analyze uncracked concrete and damage mechanics with a gradually changing elastic modulus to simulate cracked concrete. Moreover, the effects of the corrosion products penetrating into concrete pores and cracks and the displacement in the rust-concrete surface were duly considered in their model. Shodja et al. [19,20] developed a nonlinear model in which the steel, rust and concrete were assumed, respectively, to be linear isotropic, power-law and nonlinear anisotropic materials. Using this model, the volume ratio of the corrosion products inside the cracks to the volume of the cracks was determined.

In practice, reinforcing bars are usually placed near the concrete surface after providing codified nominal concrete cover to maximize the sectional moment capacity. For all the thick-walled cylinder models available in the literature [1–24], the size of the uncracked cylinder is equal to the distance measured from the center of the reinforcing bar to the nearest concrete surface that is the thinnest cover surface. All predicted results based on the thick-walled cylinder models, such as the time to cracking, the corrosion-caused expansive pressure, the width of crack and the amount of consumed iron, are obtained by solely analyzing the concrete cylinders without considering the effects of confinement pressure provided by the concrete outside the cylinders; this can, however, restrain the expansion of concrete cylinders, reduce the tensile strains developed in the cylinders, and hence slow down the cracking process of the cover. Without considering this beneficial confinement effect outside the cylinder, the predicted life of cover would be underestimated.

In this study, a double-cylinder model is developed with the consideration of the aforementioned confinement effect together with other, unique, features including: (1) accounting for the residual tensile stress in cracked concrete, (2) considering the stiffness contribution from both reinforcement and corrosion products, (3) modeling the volume compatibility condition in the steel-rust-concrete interface, and (4) simulation of the continuity of stress and strain on the common boundary between the uncracked and cracked concrete cylinders. This model is capable of predicting the time to cracking, the corrosion-caused expansive pressure and the amount of iron consumed during the corrosion-caused cracking process. A numerical parametric study has been carried out to investigate the effects of the ratio of cover thickness to reinforcing bar diameter, tensile strength of concrete, mechanical behavior and chemical composition of rust, and the volume of corrosion products diffused into the cracks on the critical volume of consumed steel, critical expansive pressure and time to cover cracking caused by corrosion.

2. The analytical model

The reinforcement corrosion problem considered in this study is illustrated in Fig. 1a. When the reinforcing bar is placed below the mid-depth of the concrete section, c_b and c_t are the thicknesses of the thinner (bottom) and thicker (top) covers, respectively. In the figure, P_{rust} is the expansive pressure caused by the deformation of the corrosion products, d_0 is the thickness of the porous zone, D is the initial diameter of the reinforcing bar embedded in the concrete, r_0 is the crack front and $t_{c,e}$ is the time to cover cracking for the actual case. The first analytical model, as shown in Fig. 1b, is the traditional model widely found in the literature in which the radius of the concrete cylinder is solely determined from the thickness of the thinner cover and is equal to $D/2 + d_0 + c_{b,0}$, where $c_{b,0} = c_b$. $P_{c,0}$ is the confining pressures provided by the uncracked concrete cylinder and $\sigma_{q,0}(r)$ is the residual tensile stresses provided by the cracked concrete cylinder. The life of concrete cover predicted by this model is likely to be underestimated as the confinement pressure outside the cylinder is ignored.

To yield a more accurate prediction, the second model, as depicted in Fig. 1c, with a cylinder radius equal to $D/2 + d_0 + c_{b,1}$ ($c_{b,1} \geq c_{b,0}$), which is larger than or equal to that of the first model, is proposed. By comparing the time to cover cracking obtained from this model to the available experimental results, the required size of the cylinder can be calibrated (details to be described in Section 4.1). The predicted results from this model, which used an enlarged concrete cylinder to account for the concrete confinement effects, are believed to better simulate real behavior. By comparing the predicted results (including cover thickness, volume of rust, corrosion-caused expansive pressure and time to cover cracking) obtained from the second model with those from the first model, a set of confinement adjustment factors (ψ_c, ψ_v, ψ_p and ψ_t all greater than or equal to 1) defined in Eqs. (1a)–(1d) can be obtained. Using this set of factors, the results of the parametric study (to be presented in Section 4.2) for the first model with a constant thickness

of concrete covers (c_b=c_t) can be extended to more realistic results for sections with unequal thicknesses of concrete covers.

$$c_{b,1} = \psi_c c_{b,0} \quad 1 \le \psi_c \tag{1a}$$

$$V_{rust,1} = \psi_v V_{rust,0} \quad 1 \le \psi_v \tag{1b}$$

$$P_{rust,1} = \psi_p P_{rust,0} \quad 1 \le \psi_p \tag{1c}$$

$$t_{c,1} = \psi_t t_{c,0} \quad 1 \le \psi_t \tag{1d}$$

where $c_{b,1}$, $V_{rust,1}$, $P_{rust,1}$ and $t_{c,1}$ are, respectively, cover thickness, volume of rust, corrosion-caused expansive pressure and time to cover cracking of the second model, whereas $c_{b,1}$, $V_{rust,0}$, $P_{rust,0}$ and $t_{c,0}$ are, respectively, cover thickness, volume of rust, corrosion-caused expansive pressure and time to cover cracking of the first model.

3. Analytical solution of the model

In the present study, the analytical solution of the generalized model representing the first model when $i = 0$ and the second model when $i = 1$ will be developed. The analytical solution for a generalized thick-walled cylinder model with a radius of $b_i = D/2 + d_0 + c_{b,i}$ ($i = 0,1$) will be obtained first, as shown in Fig. 2. The concrete with an embedded bar can be modeled as a thick-wall cylinder [1–24] and the whole cracking process caused by corrosion can be divided into four stages: the free expansion stage, the stress initiation stage (see Fig. 2a), the partial cracking stage (see Fig. 2b and c) and the completely opened cracking caused by unstable cracking (see Fig. 2d).

The analytical solution is developed by considering the following conditions: (1) the force equilibrium in the tangential direction, (2) volume expansion in the steel-rust-concrete interface, (3) deformation compatibility in the steel-rust-concrete interface, and (4) the force equilibrium in the radial direction.

3.1. Force equilibrium in the tangential direction

During the free expansion stage, a porous zone, which is caused by entrapped or entrained air that voids around the interface between steel and concrete, is assumed to exist [1]. The corrosion product can diffuse into the capillary voids in the cement paste [1,2]. After the initiation of steel corrosion, the penetration of corrosion products into the porous zone of concrete and the formation of a corrosion layer at the steel/concrete interface proceed simultaneously [25–26]. While the corrosion products penetrating into the porous zone will not generate extra stresses to the surrounding concrete and the volume increase is compensated by a filling up of the porous zone.

3.1.1. Stress initiation stage

The expansion of the corrosion products at the steel/concrete interface is restrained by the surrounding concrete. Further production of corrosion products will develop an expansive pressure $P_{rust,i}$ on the concrete, as shown in Fig. 2a. Indeed corrosion and the distribution of corrosion products in corroded rebar do not occur uniformly in practice and non-uniform corrosion around the rebar is commonly found in real situations [18]. The non-uniform corrosion problem has been studied by finite element methods [27–31] or experimental method [32]. However, for the sake of simplicity, the porous zone around the steel bar and the expansive pressure exerted on the surrounding concrete are both assumed to be uniformly distributed in the tangential direction [1,21] in this paper.

In this period, the linear elastic mechanics is employed to analyze the concrete cylinder. The stresses, strains and displacements of a thick-walled cylinder subjected to internal radial pressure can be expressed as [33]

$$\begin{cases} \sigma_{r,i}(r) = \dfrac{a^2 P_{rust,i}}{b_i^2 - a^2}\left(1 - \dfrac{b_i^2}{r^2}\right) \\ \sigma_{\theta,i}(r) = \dfrac{a^2 P_{rust,i}}{b_i^2 - a^2}\left(1 + \dfrac{b_i^2}{r^2}\right) \end{cases} \tag{2}$$

$$\begin{cases} \epsilon_{r,i}(r) = \dfrac{a^2 P_{rust,i}}{\left(b_i^2 - a^2\right) E_{c,ef}}\left(1 - \nu_c + \dfrac{\nu b_i^2}{r^2}\right) \\ \epsilon_{\theta,i}(r) = \dfrac{a^2 P_{rust,i}}{\left(b_i^2 - a^2\right) E_{c,ef}}\left[(1 - \nu_c) + (1 + \nu_c)\dfrac{b_i^2}{r^2}\right] \end{cases} \tag{3}$$

$$u_i(r) = \frac{a^2 r P_{rust,i}}{\left(b_i^2 - a^2\right) E_{c,ef}}\left[(1 - \nu_c) + (1 + \nu_c)\frac{b_i^2}{r^2}\right] \tag{4}$$

where $a = D/2 + d_0$, ν_c is the Poisson's ratio of concrete, $E_{c,ef} = E_c/(1 + \phi_{cr})$ is an effective elastic modulus of concrete, E_c is the elastic modulus of concrete, ϕ_{cr} is the creep coefficient of concrete, $\sigma_{r,i}(r)$ and $\sigma_{\theta,i}(r)$ are the radial and tangential stresses, respectively, $\epsilon_{r,i}(r)$ and $\epsilon_{\theta,i}(r)$ are the radial and tangential strains, respectively, and $u_i(r)$ is the radial deformation.

It should be noted that, in the indoor accelerated corrosion tests, as the time to cover cracking caused by the corrosion of steel bar usually only takes a few months, the elastic modulus of concrete is unaffected by aging and can be treated as a time-independent material property, i.e., $\phi_{cr} = 0$.

Then, the tangential strain of concrete in the steel-concrete interface can be expressed as

$$\epsilon_{\theta,i}(a) = \frac{a^2 P_{rust,i}}{\left(b_i^2 - a^2\right) E_{c,ef}}\left[(1 - \nu_c) + (1 + \nu_c)\frac{b_i^2}{a^2}\right] \tag{5}$$

Cracks start to occur when the tangential tensile strain at the steel-concrete interface has reached the ultimate tensile strain, that is

$$\epsilon_{\theta,i}(a) = \epsilon_{ct} \tag{6}$$

where ϵ_{ct} is the ultimate tensile strain of concrete, which can be obtained by Hooke's law $\epsilon_{ct} = f_t/E_{c,ef}$, where f_t is the tensile strength of concrete.

3.1.2. Partial cracking stage

The radial pressure increases with the increase of the corrosion products and, when the internal tensile stress in the tangential direction reaches the tensile strength of concrete, cracks are initiated from the steel-concrete interface and propagate towards the concrete cover surface. The smeared crack model is employed in this study and the average strains and stresses in the tangential direction are used in the formulation. The cracks in the concrete cylinder propagate along the radial direction and stop at $r_{0,i}$ ($a < r_{0,i} < b_i$) to reach a state of equilibrium. Thus, the thick-walled cylinder can be divided into two coaxial cylinders, the inner cracked one ($a < r < r_{0,i}$) and the outer uncracked one ($r_{0,i} < r < b_i$), as shown in Fig. 2b and c. The uncracked concrete is considered as an anisotropic linear elastic material. The tension softening effect is considered in the cracked concrete cylinder in which the tangential stiffness reduces gradually from the concrete-steel interface to the inner wall of the uncracked cylinder.

The corrosion product-induced expansive pressure $P_{rust,i}$ is resisted by the confining pressure $P_{c,i}$ developed in the uncracked concrete cylinder together with the residual tensile stress $\sigma_{\theta,i}(r)$

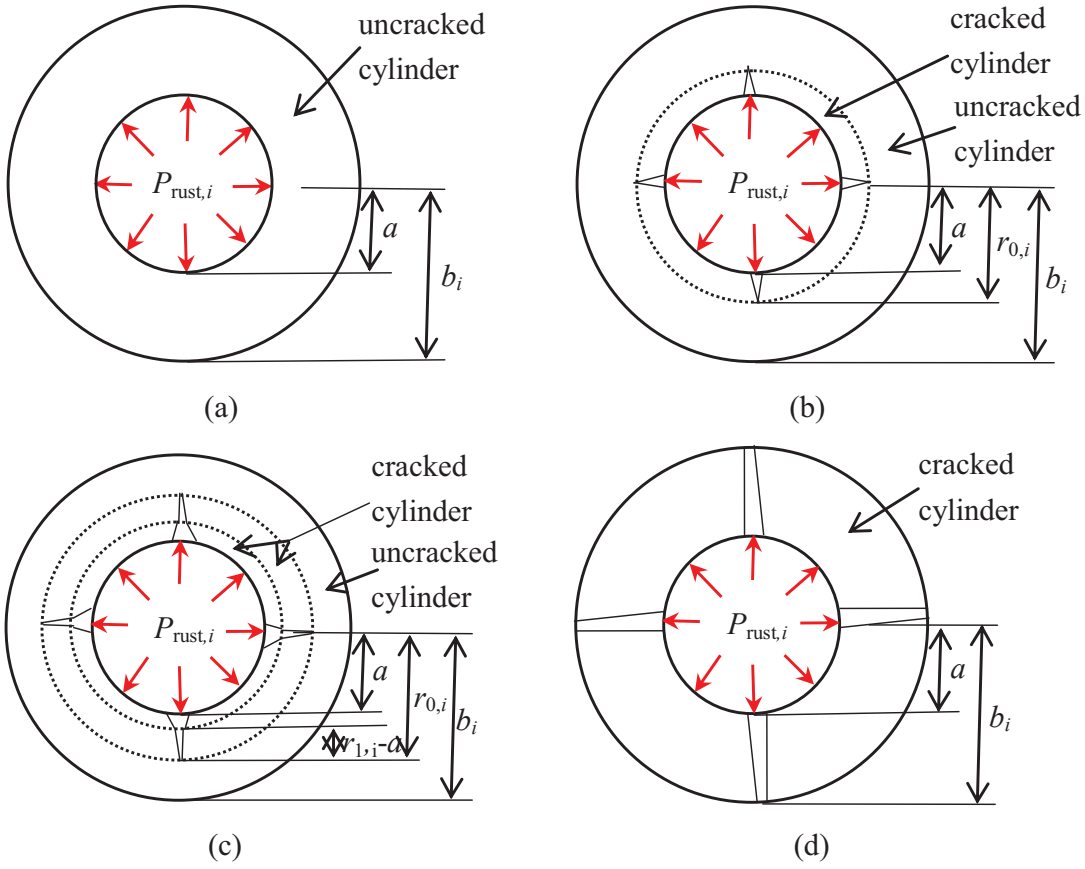

Fig. 2. Double-cylinder cracking model: (a) the stress initiation stage, (b) the first partial cracking stage, (c) the second partial cracking stage, and (d) the complete cracking stage.

provided by the cracked concrete cylinder. Thus, the force equilibrium condition can be expressed as [8–9]

$$P_{rust,i}a = P_{c,i}r_{0,i} + \int_a^{r_{0,i}} \sigma_{\theta,i}(r)\,dr \tag{7}$$

For the uncracked cylinder ($r_{0,i} \le r \le b_i$), the tangential force provided by the residual tensile stress $\sigma_{\theta,i}(r)$ is in equilibrium with the confining pressure $P_{c,i}$; hence

$$\sigma_{\theta,i}(r) = \frac{r_{0,i}^2 P_{c,i}}{b_i^2 - r_{0,i}^2}\left(1 + \frac{b_i^2}{r^2}\right) \tag{8}$$

and the boundary condition is

$$\sigma_{\theta,i}\left(r_{0,i}\right) = f_t \tag{9}$$

By equating Eq. (9) to Eq. (8), the confining pressure $P_{c,i}$ provided by the uncracked cylinder can be obtained

$$P_{c,i} = f_t \frac{b_i^2 - r_{0,i}^2}{b_i^2 + r_{0,i}^2} \tag{10}$$

Considering a bilinear softening behavior of concrete, as shown in Fig. 3, the relationship between the tangential stress and tangential strain of concrete under tension [34] can be expressed as

$$\begin{cases} \sigma_{\theta,i}(r) = E_c\epsilon_{\theta,i}(r) & \epsilon_{\theta,i}(r) \le \epsilon_{ct} \\ \sigma_{\theta,i}(r) = f_t\left[1 - 0.85 \cdot \dfrac{\epsilon_{\theta,i}(r) - \epsilon_{ct}}{\epsilon_1 - \epsilon_{ct}}\right] & \epsilon_{ct} < \epsilon_{\theta,i}(r) \le \epsilon_1 \\ \sigma_{\theta,i}(r) = 0.15f_t\dfrac{\epsilon_u - \epsilon_{\theta,i}(r)}{\epsilon_u - \epsilon_1} & \epsilon_1 < \epsilon_{\theta,i}(r) \le \epsilon_u \end{cases} \tag{11}$$

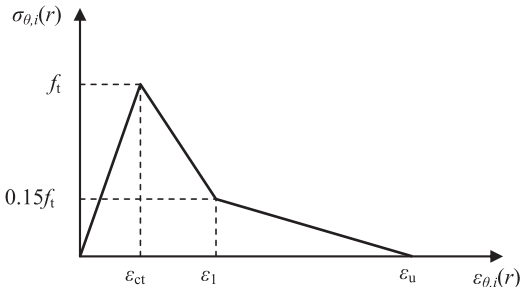

Fig. 3. Stress–strain relationship of concrete in tension.

Cracks start to occur when the tangential tensile strain at the steel-concrete interface has reached the ultimate tensile strain, ϵ_{ct}. Further expansion of the corrosion products causes the tangential tensile strain of concrete in the steel-rust-concrete interface to change from $\epsilon_{ct} < \epsilon_{\theta,i}(a) < \epsilon_1$ to $\epsilon_1 < \epsilon_{\theta,i}(a) < \epsilon_u$. Hence, the partial cracking stage can be divided into the first partial cracking stage ($\epsilon_{ct} \le \epsilon_{\theta,i}(a) \le \epsilon_1$) and the second partial cracking stage ($\epsilon_1 \le \epsilon_{\theta,i}(a) \le \epsilon_u$), as shown in Fig. 2b and c, respectively.

The bilinear softening curve is used to describe the residual tensile strength of concrete as a function of a fictitious crack opening w. The coordinates of the fictitious crack opening w_1 and w_u can be taken as $\sigma_{\theta,i}(r) = 0.15f_t$ and $\sigma_{\theta,i}(r) = 0$, respectively, in the softening curve [34]. Based on the previous test results [7,35], w_1 and w_u are approximately equal to 0.03 mm and 0.2 mm, respectively. In the present study, the corresponding strains ϵ_1 and ϵ_u are calculated based on the characteristic crack-band width h_c to account for the size effect so that $\epsilon h_c = w$. Bažant and Oh [36] suggested that h_c is approximately equal to $4d_a$, where d_a is the maximum aggregate

size, which is taken as 20 mm in this study. Therefore, $\epsilon_1 = 0.000375$ and $\epsilon_u = 0.0025$.

3.1.2.1. First stage of partial cracking ($\epsilon_{ct} \le \epsilon_{\theta,i}(a) \le \epsilon_1$). At the first stage of partial cracking, the tangential stress of concrete at radius $r_{0,i}$ is f_t and the stresses of cracked concrete are less than f_t. As the smeared crack model is employed, the total crack openings can be obtained by integrating the exceedance of the average tangential tensile strain with the cracking strain along the tangential direction of the cracked cylinder. Hence, the total crack openings $w_i(r)$ at a ring with a radius r, can be expressed as

$$2\pi r\left[\epsilon_{\theta,i}(r) - \epsilon_{ct}\right] = w_i(r) \tag{12}$$

In order to calculate the tangential stress distribution in the cracked cylinder, we assume that $w_i(r)$ decreases linearly along the radial direction from $w_i(a)$ at $r = a$ to 0 at $r_{0,i}$. Thus, the total crack openings can be expressed as

$$w_i(r) = \frac{w_i(a)\left(r_{0,i} - r\right)}{r_{0,i} - a} \tag{13}$$

Equating Eq. (13) to Eq. (12), the strain of concrete in the cracked cylinder along the radial direction can be obtained

$$\epsilon_{\theta,i}(r) = \frac{w_i(a)\left(r_{0,i} - r\right)}{2\pi r\left(r_{0,i} - a\right)} + \epsilon_{ct} \tag{14}$$

Equating Eq. (14) to Eq. (11), the confining pressure caused by the residual tensile stress $\sigma_{\theta,i}(r)$ can be obtained

$$\int_a^{r_{0,i}} \sigma_{\theta,i}(r)\,dr = f_t\left[r_{0,i} - a - \frac{0.85 w_i(a)\left(r_{0,i}\ln\frac{r_{0,i}}{a} - r_{0,i} + a\right)}{2\pi\left(r_{0,i} - a\right)(\epsilon_1 - \epsilon_{ct})}\right] \tag{15}$$

At the end of this stage, when $\sigma_{\theta,i}(a) = 0.15 f_t$, the crack opening is at $r = a$ is $w_{1,i}(a)$ and the crack front is at $r_{1,i}$, as shown in Fig. 4a. The radial distance resulting in the tangential stress in concrete decreasing from f_t to $0.15 f_t$ is $r_{1,i}$ - a.

3.1.2.2. Second stage of partial cracking ($\epsilon_1 \le \epsilon_{\theta,i}(a) \le \epsilon_u$). In the second stage of partial cracking, we assume that the radial distance resulting in the tangential stress of concrete decreasing from f_t to $0.15 f_t$ is the same as that for the first stage of partial cracking (see Fig. 4) when the crack is continuously penetrating into the concrete. The continuity of stress and strain on the common boundary between the uncracked and cracked concrete cylinders is maintained. The total crack openings at radius $r_{0,i}$-$r_{1,i}$+a at the second stage of partial cracking and at radius a at the first stage of partial cracking are expressed in Eqs. (17) and (16) respectively.

$$w_{1,i}\left(r_{0,i} - r_{1,i} + a\right) = 2\pi\left(r_{0,i} - r_{1,i} + a\right)(\epsilon_1 - \epsilon_{ct}) \tag{16}$$

$$w_{1,i}(a) = 2\pi a(\epsilon_1 - \epsilon_{ct}) \tag{17}$$

By equating the strains at radius $r_{0,i}$-$r_{1,i}$ + a at the second stage of partial cracking and at radius a at the first stage of partial cracking, and using Eqs. (17) and (16), one can have

$$w_{1,i}\left(r_{0,i} - r_{1,i} + a\right) = \frac{\left(r_{0,i} - r_{1,i} + a\right) w_{1,i}(a)}{a} \tag{18}$$

As shown in Figs. 2c and 4b, the cracked cylinder is divided into two parts: the inner cracked part ($a \le r \le r_{0,i}$-$r_{1,i}$ + a) and the outer cracked part ($r_{0,i}$–$r_{1,i}$ + $a \le r \le r_{0,i}$). In order to calculate the tangential stress distribution in the cracked cylinder, it is assumed that the total crack openings $w_i(r)$ decrease linearly in the two parts, respectively, along the radial direction. Therefore, the total crack openings along the wall of the cracked cylinder can be expressed as

$$\begin{cases} w_i(r) = \dfrac{w_i(a)\left(r_{0,i} - r_{1,i} + a - r\right) + w_{1,i}\left(r_{0,i} - r_{1,i} + a\right)(r - a)}{r_{0,i} - r_{1,i}} & a \le r \le r_{0,i} - r_{1,i} + a \\ w_i(r) = \dfrac{w_{1,i}\left(r_{0,i} - r_{1,i} + a\right)\left(r_{0,i} - r\right)}{r_{1,i} - a} & r_{0,i} - r_{1,i} + a \le r \le r_{0,i} \end{cases} \tag{19}$$

By equating Eqs. (19) and (12), the strain of concrete in the tangential direction in the cracked cylinder can be obtained

$$\begin{cases} \epsilon_{\theta,i}(r) = \dfrac{w_i(a)\left(r_{0,i} - r_{1,i} + a - r\right) + w_{1,i}\left(r_{0,i} - r_{1,i} + a\right)(r - a)}{2\pi r\left(r_{0,i} - r_{1,i}\right)} + \epsilon_{ct} & a \le r \le r_{0,i} - r_{1,i} + a \\ \epsilon_{\theta,i}(r) = \dfrac{w_{1,i}\left(r_{0,i} - r_{1,i} + a\right)\left(r_{0,i} - r\right)}{2\pi r\left(r_{1,i} - a\right)} + \epsilon_{ct} & r_{0,i} - r_{1,i} + a \le r \le r_{0,i} \end{cases} \tag{20}$$

By equating Eqs. (20) and (11), the confining pressure developed by the residual tensile stress $\sigma_{\theta,i}(r)$ can then be obtained

$$\int_a^{r_{0,i}} \sigma_{\theta,1}(r)dr = \frac{0.15 f_t}{\epsilon_u - \epsilon_1}\left\{(\epsilon_u - \epsilon_{ct})(r_{0,i} - r_1) + \frac{w_i(a) - w_{1,i}(r_{0,i} - r_{1,i} + a)}{2\pi} - \frac{1}{2\pi}\left[w_i(a) + a \times \frac{w_i(a) - w_{1,i(r_{0,i} - r_{1,i} + a)}}{r_{0,i} - r_{1,i}}\right]\ln\frac{r_{0,i} - r_{1,i} + a}{a}\right\}$$
$$+ f_t\left[(r_{1,i} - a) - 0.85 \times \frac{w_{1,i}(r_{0,i} - r_{1,i} + a)\left(r_{0,i}\ln\frac{r_{0,i}}{r_{0,i} - r_{1,i} + a} - r_{1,i} + a\right)}{2\pi(r_{1,i} - a)(\epsilon_1 - \epsilon_{ct})}\right] \tag{21}$$

3.1.3. Unstable cracking

As the expansive pressure increases, cracks propagate unstably through the cover when the value of the expansive pressure reaches the maximum value. Cracks would then appear on the surface of concrete cover (see Fig. 2d).

3.2. Volume expansion in the steel-rust-concrete interface

In the stress initiation stage, the net volume of corrosion product $V_{net,i}$ which causes pressure on the surrounding concrete is summarized as follows

$$V_{net,i} = V_{rust,i} - V_{steel,i} - V_{porous,i} \tag{22}$$